Immunity
Article

Unique Maturation Program of the IgE Response In Vivo

Agustin Erazo,[1] Nino Kutchukhidze,[1] Monica Leung,[1,2] Ana P. Guarnieri Christ,[4] Joseph F. Urban, Jr.,[5] Maria A. Curotto de Lafaille,[1,3,*] and Juan J. Lafaille[1,3,*]
[1] Program of Molecular Pathogenesis, Skirball Institute of Biomolecular Medicine
[2] Sackler Institute of Graduate Biomedical Sciences
[3] Department of Pathology
New York University School of Medicine, New York, NY 10016, USA
[4] Departmento de Imunologia, Universidade de São Paulo, São Paulo CEP: 05508-900, Brasil
[5] Nutrient Requirements and Functions Laboratory, Beltsville Human Nutrition Research Center, Agricultural Research Service, USDA, Beltsville, MD 20705, USA
*Correspondence: curotto@saturn.med.nyu.edu (M.A.C.de L.), lafaille@saturn.med.nyu.edu (J.J.L.)
DOI 10.1016/j.immuni.2006.12.006

SUMMARY

A key event in the pathogenesis of asthma and allergies is the production of IgE antibodies. We show here that IgE$^+$ cells were exceptional because they were largely found outside germinal centers and expressed, from very early on, a genetic program of plasma cells. In spite of their extragerminal center localization, IgE$^+$ cells showed signs of somatic hypermutation and affinity maturation. We demonstrated that high-affinity IgE$^+$ cells could be generated through a unique differentiation program that involved two phases: a pre-IgE phase in which somatic hypermutation and affinity maturation take place in IgG1$^+$ cells, and a post-IgE-switching phase in which IgE cells differentiate swiftly into plasma cells. Our results have implications for the understanding of IgE memory responses in allergy.

INTRODUCTION

IgE antibodies are major contributors to pathology in atopic diseases (Oettgen and Geha, 2001). In mice, both IgE and IgG1 antibodies are generated during T cell-dependent B cell responses mediated by T helper 2 (Th2) lymphocytes (Coffman et al., 1993). However, IgE responses are strictly dependent on interleukin-4 (IL-4), whereas, under some circumstances, IgG1 antibodies can be found in mice treated with anti-IL-4 and in IL-4 or signal transducer and activator of transcription-6 (STAT6)-deficient mice (Finkelman et al., 1988; Kaplan et al., 1996; Kuhn et al., 1991; Shimoda et al., 1996). IL-18 administration (in the absence of IL-12) has also been shown to induce IgE production, through an IL-4-STAT6-dependent mechanism (Hoshino et al., 2000; Yoshimoto et al., 2000).

In T cell-dependent responses, IgG1$^+$ cells can be found in in germinal centers (GCs), which are the follicular structures where class switch recombination (CSR), somatic hypermutation (SHM), and affinity maturation take place. GCs are essential for the formation of memory B cells and long-lived plasma cells (Przylepa et al., 1998).

Despite the importance of the IgE response, little is known about the location of switching to IgE, the biology of IgE$^+$ cells, and even whether memory IgE$^+$ cells exist. One of the reasons for the limited amount of information that is available is that the study of the biology of IgE$^+$ cells and their tracking in vivo is hampered by their low frequency, even in the favorable conditions of Th2 responses. To circumvent this problem, we used two mouse models of high IgE production in vivo: immunization-driven hyper IgE response in mice with monoclonal T and B cells (T/B monoclonal mice) and helminth infection IgE induction in BALB/c mice.

In the present work, we showed that high-affinity IgE antibodies could be generated in a nonconventional manner. Switching to IgE initiated in the GC, but IgE$^+$ cells differentiated quickly into plasma cells and were mostly found outside GC areas. In spite of their brief GC phase, IgE antibodies displayed somatic hypermutation and affinity maturation. We demonstrated that purified GC IgG1$^+$ and memory IgG1$^+$ cells could undergo a secondary switch to IgE in a process that required IL-4 and was inhibited by IL-21. We propose a model whereby high-affinity IgE antibodies are generated through sequential switching of IgG1$^+$ B cells, without the need for a genuine memory IgE$^+$ cell compartment.

RESULTS

IgE$^+$ Cells Are Found outside GC

In order to characterize the generation and maturation of IgE$^+$ cells, we used two mouse models of high IgE response. High IgE production was elicited either by immunization of T/B monoclonal mice (Curotto de Lafaille et al., 2001) or by infection of wild-type BALB/c mice with the helminth parasite *Nippostrongylus brasiliensis* (Finkelman et al., 1990; Katona et al., 1988). T/B monoclonal mice carry anti-chicken ovalbumin (OVA) T cell receptor transgenes (DO11.10) and anti-influenza hemagglutinin (HA)

knockin B cell receptor genes on a RAG1-deficient background. The use of T/B monoclonal mice enables the tracking of antigen-specific B cells, whereas the helminth infection of wild-type mice allows us to analyze a broad repertoire response in a nonmanipulated immune system.

We first characterized the temporal and spatial appearance of IgG1$^+$ and IgE$^+$ cells, as well as GL7$^+$ GC cells, in peripheral lymphoid organs of T/B monoclonal mice after immunization with the cognate antigen OVA-HA in alum. No or very few IgG1 or IgE-producing cells or IgE antibodies were observed when T/B monoclonal mice were immunized with Alum only or myelin basic protein (MBP) in alum (see Figure S1 in the Supplemental Data available online). Although a substantial response was attained by immunization with OVA in Alum, the highest response occurred, as expected, when mice were immunized with the crosslinked OVA-HA antigen (Figure S1). Upon immunization with OVA-HA, GC cells were barely detectable in spleen and mesenteric LN 6 days after immunization, but increased rapidly thereafter (Figure 1A and Figure S2). Appearance of IgG1$^+$ and IgE$^+$ cells paralleled GC formation, as assessed by surface staining (Figure 1A) or mRNA analysis (Figure S3). Our results correlate well with the kinetics of serum IgG1 and IgE responses elicited by anti-IgD treatment of wild-type mice (Finkelman et al., 1989). IgG1 and IgE production followed the increase in IL-4 production, consistent with the Th2 dependence of these two isotypes (Figure S3).

The localization of IgG1$^+$ and IgE$^+$ cells in sections of mesenteric LN and spleen was determined by immunohistochemistry (Figure 1B and Figure S4). GC cells are B220$^+$, IgD$^-$, Fas$^+$ and bind the GL7 antibody and the lectin PNA. In Figures 1 and 2, GC were identified as IgD$^-$ follicular areas or by staining with the GL7 antibody. T cell areas were identified with TCRβ antibodies. As anticipated, IgG1$^+$ cells occupied the GC areas, and some were also found in the T cell areas and red pulp in the spleen and in the medullary region of LN (Figure 1B and Figure S4). Unexpectedly, the vast majority of IgE$^+$ cells were not found inside GC in LN of immunized mice. Instead, IgE$^+$ cells were found at the boundaries of GC and T cell areas, in non-GC B cell areas, and in medullary cords (Figure 1B). In spleen, IgE$^+$ cells localized to the boundaries of T and B cell areas and to T cell areas and were largely absent from follicles and GC (Figure S4). A thorough kinetic analysis of appearance of IgE$^+$ cells showed that their absence from GC was not a matter of the times chosen for analysis (Figure S4).

IgE$^+$ cell localization was also analyzed during the GC phase of the response of wild-type BALB/c mice to infection with the helminth *Nippostrongylus brasiliensis*. Similarly to T/B monoclonal mice, most IgE$^+$ cells were found outside GC areas, in non-GC IgD$^+$ B cell areas, including the medullary region (Figures 2A and 2B), whereas IgG1$^+$ cells were found mainly in GC (Figure 2C). The morphology of IgG1$^+$ and IgE$^+$ cells also differed, with IgE$^+$ cells displaying a plasmablast morphology (Figure 2D). The kinetic analysis of the IgG1 and IgE responses in *Nippostrongylus brasiliensis*-infected mice is provided in Figure S5.

GC Origin of ε Sterile Transcripts

The absence, at all time points, of IgE$^+$ cells in GC of animals undergoing high IgE responses in both animal models was unexpected. To analyze class switching to IgE in GC and non-GC cells at the molecular level, we tracked the expression of IgE-specific transcripts: (1) ε sterile transcript, which is transcribed from the Iε promoter, precedes and is essential for CSR to IgE; (2) ε postswitched transcript, which originates from the Iμ promoter after CSR to ε took place (labeled "Switched transcript" in Figure 3A); and (3) ε mature transcript, which is transcribed from the VDJ promoter (Li et al., 1994; Rothman et al., 1988; Stavnezer et al., 1988). IgG1$^+$ GC cells (B220$^+$PNA$^+$IgG1$^+$), IgG1$^-$ GC cells (B220$^+$PNA$^+$IgG1$^-$), plasma cells (Syndecan-1$^+$), and non-GC non-plasma cell B cells (B220$^+$PNA$^-$Syn$^-$) were purified from spleen of mice on day 12 of immunization. Expression of ε transcripts in the fractions was analyzed by real-time PCR (Figure 3B). The highest expression of ε sterile transcripts was found in the two GC (PNA$^+$) fractions, indicating that switching to IgE initiates in the GC. Postswitched ε transcripts predominated in the PNA$^+$IgG1$^+$ fraction of GC. Mature ε transcripts were found in the PNA$^+$IgG1$^-$ fraction but not in the PNA$^+$IgG1$^+$ fraction. The highest expression of mature IgE transcripts was detected in the Syndecan-1$^+$ fraction. Although sterile and postswitched transcripts could be derived from the second chromosome, which has the VDJ gene segments in germline configuration in these RAG-deficient mice, the very low amount of sterile transcript in non-GC B220$^+$ cells supports the GC origin of IgE switching. In sum, the kinetics shown in Figure 1A and the pattern of expression of sterile ε transcripts indicates that class switching to IgE initiates in GC.

Swift Differentiation of IgE$^+$ Cells into Plasma Cells

To determine the differentiation state of IgE$^+$ cells during the GC phase of a primary response, we analyzed the expression of Syndecan-1, Fas, and B220 in IgE$^+$ (and IgG1$^+$) cells in mesenteric LN from immunized T/B monoclonal mice and *Nippostrongylus brasiliensis*-infected BALB/c mice. Most IgE$^+$ cells did not express B220 and expressed high amounts of Fas, and a large fraction (80.9% ± 6.3% in T/B monoclonal mice and 57.2% ± 11.5% in *Nippostrongylus*-infected BALB/c mice) expressed Syndecan-1 (Figure 4A). Loss of B220 expression and acquisition of Syndecan-1 expression are characteristic of plasma cells. In contrast, most IgG1$^+$ cells were B220$^+$Fas$^+$Syndecan-1$^-$ (96.8% ± 0.9% in T/B monoclonal mice and 94.5% ± 0.5% in *Nippostrongylus*-infected BALB/c mice), consistent with their GC localization (Figure 4A, see overlapping histograms of gated IgE$^+$ and IgG1$^+$ cells). Analysis of gated Syndecan-1$^+$ cells showed an overrepresentation of surface IgE$^+$ cells (20%–40%) in this fraction (Figure 4B). The validity of the identification of IgE$^+$ and IgG1$^+$ cells was confirmed by the expression of mature IgE and IgG1 transcripts, respectively (Figure 4C). As expected, there were very few IgE$^+$ and IgG1$^+$ cells, as well as Syndecan$^+$ cells, in unimmunized T/B monoclonal mice or untreated BALB/c mice (Figure 4D). The localization of IgE$^+$

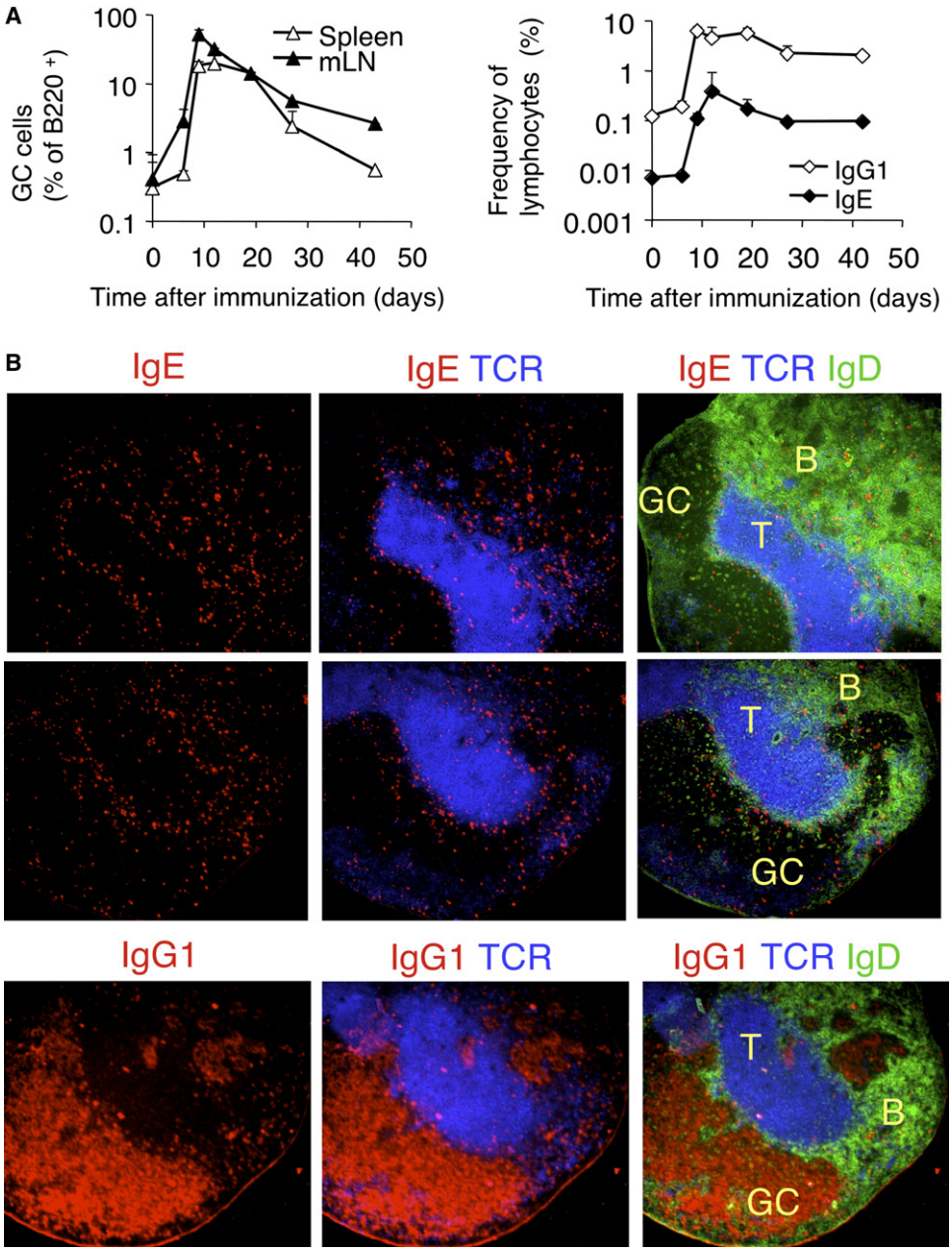

Figure 1. Switching to IgE Occurs during the GC Phase of an Immune Response, but IgE Cells Are Found outside GC

T/B monoclonal mice were immunized with OVA-HA in alum by i.p. route.

(A) Kinetics of appearance of GC ($GL7^+B220^+$) in spleen and mesenteric LN (mLN) and of IgE^+ and $IgG1^+$ cells in mLN. Shown are mean ± SD. n = 3 mice per time point. The data were derived from FACS analysis of cells on days 6, 9, 12, 19, 27, and 43 after primary immunization, with the gates shown in Figure S1. Representative of three experiments.

(B) Immunohistochemistry showing tissue distribution of IgE^+ and $IgG1^+$ cells in sections of mLN at day 12 of immunization. Germinal centers (GC), T cell, and follicular B cell (B) areas are indicated. Original magnification 100×. More than 100 sections from 30 mice were analyzed.

cells and their pattern of B220 and Syndecan expression suggested a plasma cell phenotype. We therefore analyzed purified IgE^+ cells for the transcription of molecules expressed at the GC stage such as Pax5 (Gonda et al., 2003; Johnson and Calame, 2003) and Bcl6 (Dent et al., 1997; Ye et al., 1997), or the plasma cell stage such as Blimp1 (Johnson and Calame, 2003) and Xbp1 (Reimold et al., 2001), as well as the enzyme AID (Muramatsu et al., 2000), required for immunoglobulin class switch recombination and somatic hypermutation. IgE^+Fas^+ cells from spleen did not express Pax5, Bcl6, or AID, but expressed high amounts of Blimp and Xbp1 (Figure 4E). The reverse was observed for the $IgG1^+$ cells. In non-GC $B220^+$ cells from immunized mice and B cells from nonimmunized

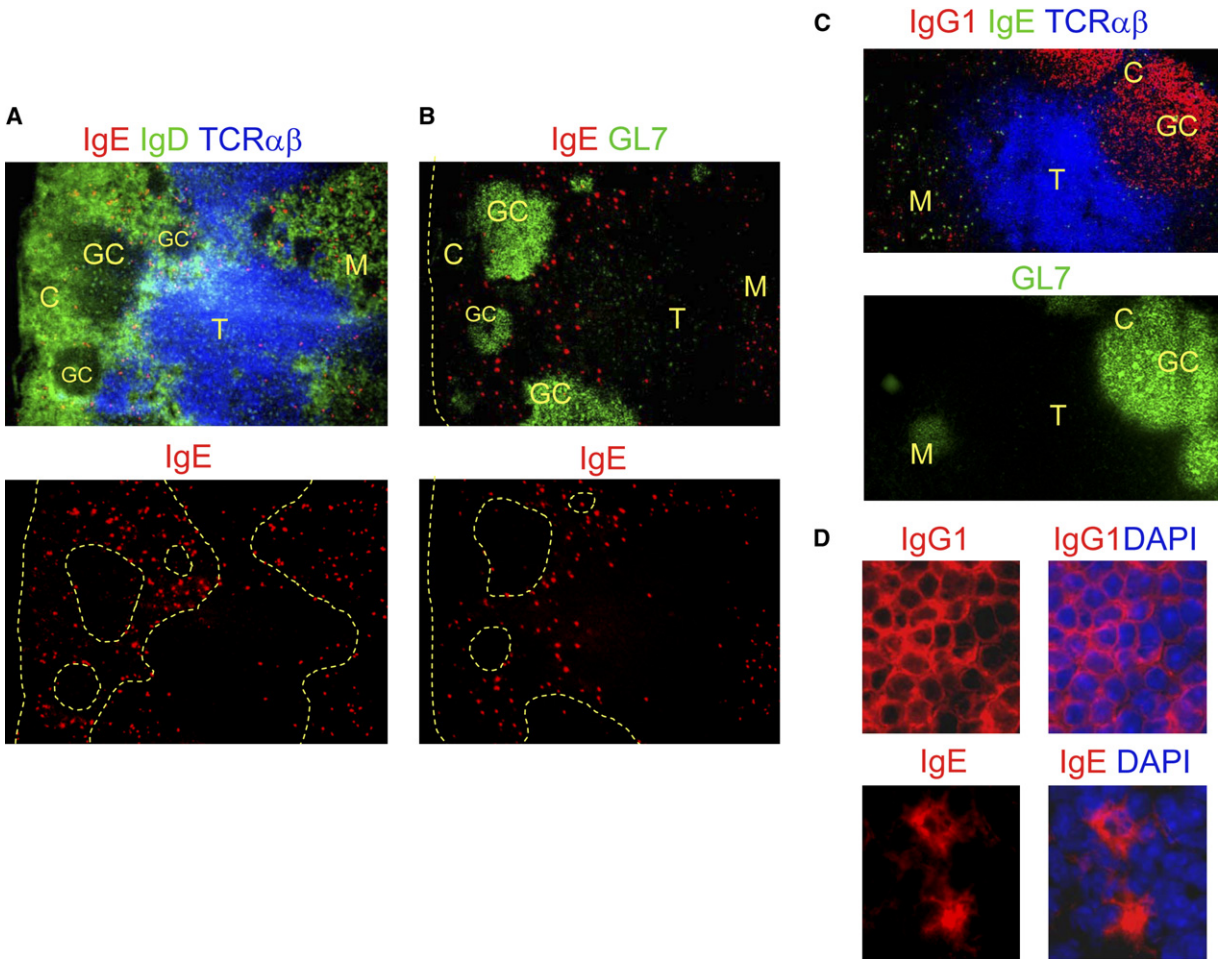

Figure 2. Different Localization of IgE$^+$ and IgG1$^+$ Cells in Lymph Nodes of BALB/c Mice Infected with *Nippostrongylus brasiliensis*

Frozen sections of mesenteric LN from *N. brasiliensis*-infected BALB/c mice (day12) were analyzed by immunohistology.
(A) Staining with antibodies to IgE, IgD, and TCRαβ reveals IgE$^+$ cells in non-GC B cell areas and medullary region.
(B) IgE$^+$ cells are found in the margins and outside GL7$^+$ GC areas.
(C) IgG1 cells colocalize with GL7$^+$ GC areas. Serial sections of the same LN are shown.
(D) IgG1$^+$ cells show predominantly membrane staining in GC, while IgE$^+$ cells have bright cytoplasmic staining.
(A, B, C) Original magnification 100×; (D) 400×. Germinal centers (GC), T cell (T), cortical (C), and medullary (M) areas are indicated. Representative of 12 mice from 2 independent experiments.

mice, only Pax5 was highly expressed, consistent with a naive phenotype. Similar results were obtained with purified IgE$^+$ and IgG1$^+$ cells from lymph nodes (LN, Figure 4E). Furthermore, we took advantadge of the fact that plasma cells, but not mature B cells, display very high fluorescence intensity after intracellular staining with anti-immunoglobulin reagents. Although only a very small percentage of the IgG1$^+$ population showed a very high fluorescence intensity upon intracellular staining, the vast majority of the IgE$^+$ population did (Figure S6). Finally, immunohistology showed that IgE$^+$ cells, but not IgG1$^+$ cells, have a morphology and cytoplasmic immunoglobulin expression characteristic of plasma cells (Figure 2D). All these results demonstrate that IgE$^+$ cells display, from early on, a genetic program of plasma cells.

It has been shown in chimeric mice that contained B cells from wild-type and *Cxcr5*$^{-/-}$ mice that B cells from the latter were excluded from GC (Allen et al., 2004). Our observation of extrafollicular localization of IgE$^+$ in spleen and of their overall exclusion from GC areas suggested the possibility of a distinct homing pattern that could involve altered regulation of CXCR5 (Allen et al., 2004; Cyster, 1999). Strikingly, no CXCR5 expression was detected in IgE$^+$ cells from spleen, likely explaining the paucity of these cells in follicular and GC areas. CXCR5 expression was also decreased in LN IgE$^+$ cells compared to IgG1$^+$ cells (Figure 4E). Thus, together with a swift differentiation to plasma cells, IgE$^+$ cells are characterized by low expression of the chemokine receptor required for follicular and GC localization.

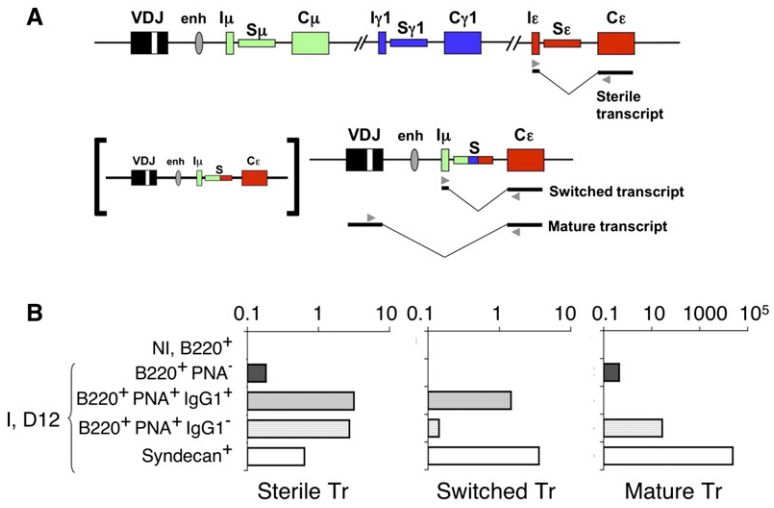

Figure 3. Class Switching to IgE Initiates in GC

(A) Schematic representation (not in scale) of the Ig heavy chain locus and the main ε transcripts, showing the localization of PCR primers (arrowheads) used to amplify ε sterile, postswitched, and mature transcripts. Exons and introns in C regions not depicted. Top scheme: DNA configuration before switching; bottom schemes: DNA configuration after switching. The bracketed scheme on the left represents an alternative result of sequential switching (without γ1 remnants) as well as the result of direct μ to ε switching.

(B) Distribution of ε sterile, switched, and mature transcripts in GC ($B220^+PNA^+IgG1^+$ and $B220^+PNA^+IgG1^-$), non-GC ($B220^+PNA^-$), and plasma cell ($Syndecan\text{-}1^+$) fractions from spleen of T/B monoclonal mice on day 12 of immunization. NI, $B220^+$: purified $B220^+$ cells from untreated T/B monoclonal mice. Expression was determined by quantitative real-time PCR. Similar results were obtained when GC and non-GC B cells were sorted based on expression of Fas, B220, and IgG1 (not shown).

Switched Cells Coexpressing IgG1 and IgE on the Cell Surface Display a Plasma Cell Phenotype

Switching to IgE and IgG1 is regulated similarly by Th2 cytokines and many costimulatory molecules. It has been shown that class-switch recombination shows no allelic exclusion (Rabbitts et al., 1980). Thus, in homozygous VDJ heavy chain knockin mice, it may be possible to detect IgG1 and IgE dual-expressing B cells. Such cells were not found in heterozygous animals (Figures 4A and 4D, Figure S1). We sought to determine whether the $IgG1^+IgE^+$ dual-expressing cells would have a GC phenotype, as do $IgG1^+$ cells, or a plasma cell phenotype, as do IgE^+ cells.

Homozygous heavy chain knockin T/B monoclonal mice were immunized with OVA-HA, and their LN cells were analyzed by flow cytometry. We found $IgG1^+IgE^+$ dual-expressing cells in similar numbers as IgE^+ single-expressing cells (Figure 5A). FACS analysis of the expression of B220, Fas, and Syndecan-1 on gated dual-expressing and single-expressing cells showed clearly that $IgG1^+IgE^+$ dual-expressing cells have a plasma cell phenotype, similar to single IgE^+ cells but unlike single-expressing $IgG1^+$ cells (Figure 5A). We then sorted $IgG1^+IgE^+$ dual-expressing cells and analyzed the expression of Pax5, Bcl6, AID, Blimp1, and Xbp1 by real-time PCR. $IgG1^+IgE^+$ dual-expressing cells displayed characteristics of plasma cells, very similar to IgE^+ single-expressing cells (Figure 5B). Analysis of mature IgG1 and IgE transcripts confirmed at the mRNA level the dual-expression status of the $IgG1^+IgE^+$ sorted cells (Figure 5B). These data show that the strong association between class switching to IgE and plasma cell differentiation cannot be overcome by expression of a functional IgG1 molecule on IgE^+ cells.

IgE Antibodies Undergo Somatic Hypermutation and Affinity Maturation

The lack of GC localization of IgE^+ cells, together with their low or absent Bcl6 and AID expression, raised the question of whether IgE antibodies undergo somatic hypermutation and affinity maturation. To study affinity maturation of IgE^+ cells, T/B monoclonal mice were repeatedly immunized with OVA coupled to a low-affinity variant of HA, named PEP1. PEP1 carries Phe in place of Tyr105 (PEP1: YPYDVPDFASLRS), a replacement that greatly reduces affinity for the knockin B cell receptor-encoded antibody (Pinilla et al., 1993; Schulze-Gahmen et al., 1993). At the concentrations used, monovalent biotinylated PEP1 does not bind to naive HA-specific B cells, whereas monovalent biotinylated HA binds virtually all B cells in these mice. However, after secondary immunization with OVA-PEP1, but not with OVA-HA, PEP1-binding cells were detected in the spleen of immunized mice (Figure S7). To identify the mutations that confer high-affinity binding to PEP1, PEP1-binding memory B cells ($PEP1^+B220^+IgD^-$) were purified from immunized mice, and the DNA sequences of VDJ IgG1 genes in the samples was determined. High-affinity binding to PEP1 correlated with a pattern of two amino acid replacements in the CDR3 region: R97T and N100aS, with a third one, A101T, appearing less frequently. These replacements were rare in IgG1 sequences from $PEP1^-B220^+IgD^-$ cells (Figure S8).

Having established which somatic mutations correlated with the appearance of binding to PEP1, we analyzed the accumulation of high-affinity amino acid replacements in IgG1 and IgE antibody genes during repeated immunization of T/B monoclonal mice with OVA-PEP1. Antibody titers of both PEP1-specific IgG1 and IgE increased with time, with the plateau in IgE titers lagging behind the

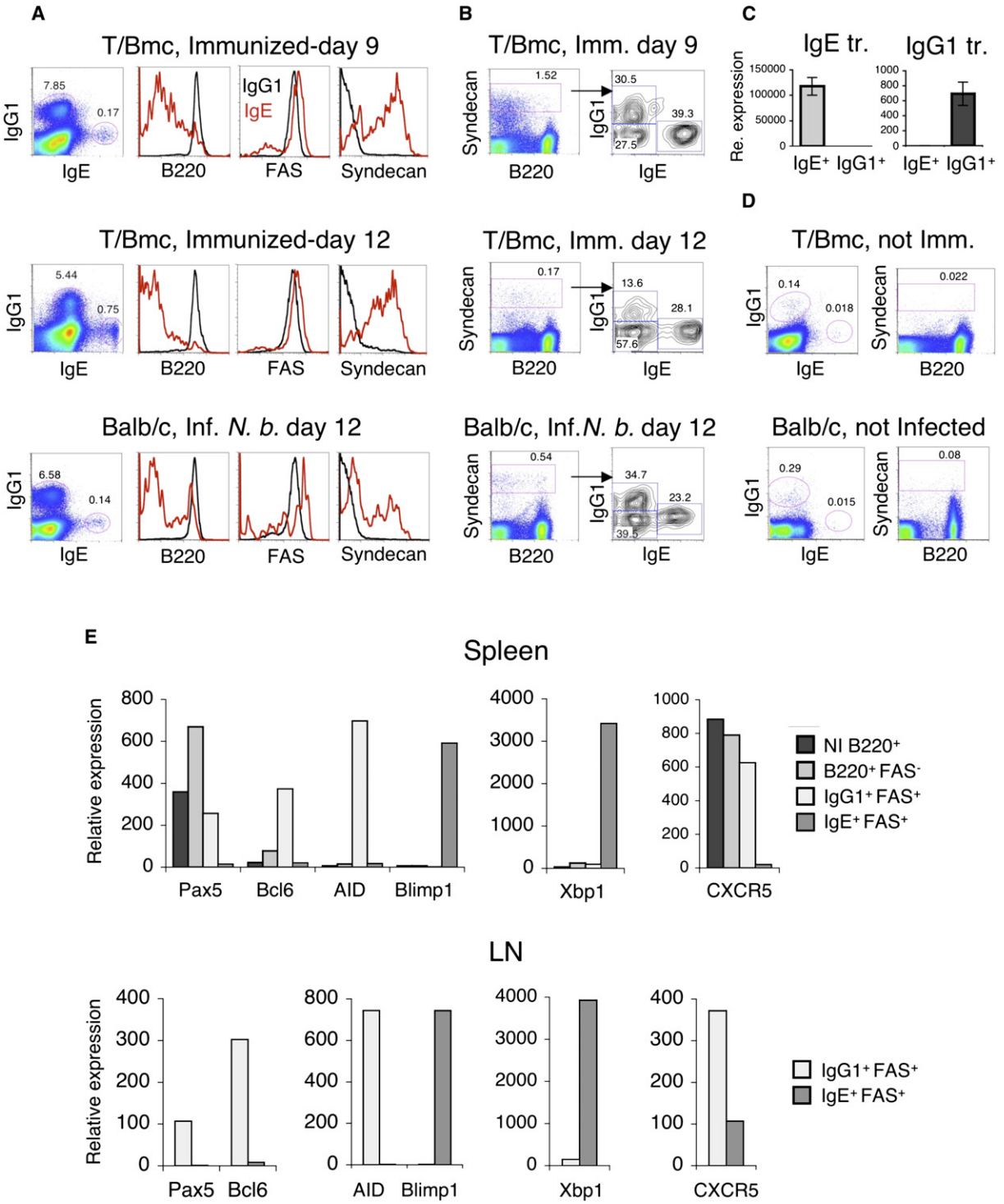

Figure 4. IgE$^+$ Cells Differentiate Swiftly into Plasma Cells

(A and B) FACS analysis of mLN cells from OVA-HA-immunized T/B monoclonal mice and *Nippostrongylus brasiliensis*-infected BALB/c mice. LN cells were acid treated to remove cytophilic (extrinsic) antibodies and subsequently stained with antibodies to IgE, IgG1, B220, and either CD95 (Fas) or Syndecan-1.

(A) Dot plots show IgE and IgG1 expression in cells from a live lymphocyte (FSC X SSC) gate. Overlay histograms show expression of B220, Fas, and Syndecan-1 in gated IgE$^+$ (red) or IgG1$^+$ (black) cells. Representative of 3 experiments with 3 mice per group.

(B) Dot plots on the left show Syndecan-1 and B220 staining of cells from a lymphocyte gate. Plots on the right show IgG1 and IgE cells among gated Syndecan-1$^+$ cells. Numbers in the quadrants show the percentage of cells.

(C) Real-time PCR analysis of mature IgE and IgG1 transcripts in IgE$^+$ and IgG1$^+$ sorted cells.

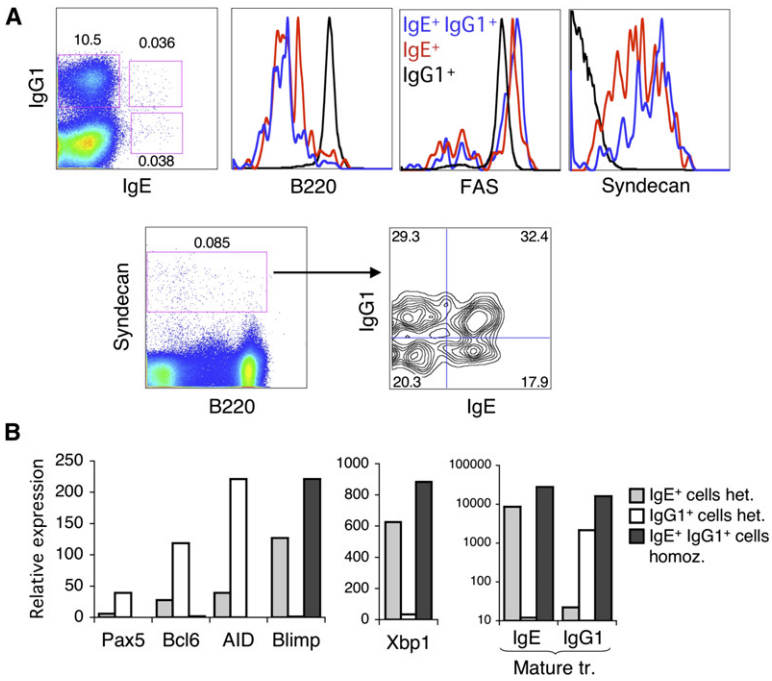

Figure 5. B Lymphocytes Coexpressing Surface IgG1 and IgE Molecules Display a Plasma Cell Phenotype

T/B monoclonal mice carrying homozygous copies of the knockin VDJ heavy and light immunoglobulin genes were immunized i.p. with OVA-HA in alum.

(A) FACS analysis of LN cells 10 days after immunization.

(B) IgG1$^+$IgE$^+$ double-expressing cells from homozygous T/B monoclonal mice and IgE$^+$ and IgG1$^+$ single-expressing cells from heterozygous mice were purified by flow cytometry sorting 15 days after immunization. The expression of Pax5, Bcl6, AID, Blimp1, Xbp1, IgG1, and IgE was determined by real-time PCR. Note the logarithmic scale for the Ig gene expression data. Representative of 2 independent experiments.

plateau of IgG1 titers (Figure 6A). IgG1 and IgE VDJ gene sequences were analyzed 10 days after the second and fourth immunization. IgG1 and IgE sequences in OVA-PEP1-immunized mice showed increased frequency of the amino acid replacement at positions R97, N100a, and A101 that correlate with high-affinity binding to PEP1 (Figure 6B). However, a frequency of high-affinity mutations comparable to IgG1 was attained in IgE molecules only after more rounds of immunization (Figure 6B). In mice immunized with the high-affinity ligand OVA-HA, we observed increased number of DNA mutations over time (Figure 6C and Figure S9), but no positive selection for particular amino acid mutations were identified, consistent with published results on other high-affinity responses (Shih et al., 2002). In contrast to IgG1 and IgE, IgG3 antibodies carried a very low number of mutations under these experimental conditions (Figure 6C and Figure S9). This is consistent with switching to IgG3 occurring mostly before the onset of the GC reaction in the response to OVA-HA (Figure S3). We conclude that, despite the lack of GC localization of IgE$^+$ cells, IgE antibodies undergo SHM and affinity maturation.

IgG1$^+$ Lymphocytes Can Generate IgE Antibodies by Sequential Switching

Our results demonstrate that high-affinity IgE antibodies are produced during a Th2-mediated response in vivo, yet a GC phase for IgE$^+$ cells could not be visualized. Based on these results and on previous findings of IgG1 switch-region remnants on IgE$^+$ cells, which demonstrated sequential switching from μ to γ1 to ε (Yoshida et al., 1990), we hypothesized that IgE$^+$ cells may not undergo somatic hypermutation and affinity maturation, but rather they could inherit mutated and selected VDJ genes from precursor IgG1$^+$ cells. Although molecular evidence supporting the existence of sequential switching is abundant, it is equally clear that sequential switching is not obligatory for IgE responses (Jung et al., 1994). Furthermore, it was possible that the second step of sequential switching (γ1 to ε) occurred very soon after the first step (μ to γ1) at a stage in which both γ1 and ε sterile transcripts are abundant, without involving an IgG1$^+$ cellular phase. To test whether or not GC or memory IgG1$^+$ cells could give rise to IgE$^+$ cells by sequential switching in vivo, we sorted B220$^+$Fas$^+$IgG1$^+$IgD$^-$ and B220$^+$Fas$^+$IgG1$^-$IgD$^-$ cells from mice immunized with OVA-PEP1. These cells were then transferred together with naive OVA-specific CD4$^+$ T cells into TCR$\alpha\beta$-deficient mice, and the recipient mice were immunized once with OVA-PEP1. Anti-PEP1 and anti-HA responses were monitored by ELISA in sera from immunized recipient mice. A PEP1-specific IgE response could be detected only in sera from mice that received the IgG1$^+$ population (Figure 7A). Similar results were obtained with *Rag1*$^{-/-}$ recipient mice (Figure S10). In the recipient mice, IgE molecules that, given the experimental design, must be derived from the transferred IgG1$^+$ cells, carried the PEP1-binding T97-S100a-T101 mutations (Figure 7B), although at lower frequency than

(D) Dot plots of gated live lymphocytes from untreated T/B monoclonal and BALB/c mice.

(E) IgE$^+$ cells express genes of the plasma cell stage. IgE$^+$Fas$^+$ cells, IgG1$^+$Fas$^+$ cells, and B220$^+$Fas$^-$ cells were sorted from spleen and mesenteric LN of T/B monoclonal mice 12 days after immunization with OVA-HA. Naive B220$^+$ cells (NI B220$^+$) were purified from spleen of untreated T/B monoclonal mice. Gene expression analysis by real-time PCR of Blimp 1, Xbp1, Pax5, Bcl6, AID, and CXCR5 is shown. Representative of four independent experiments.

A

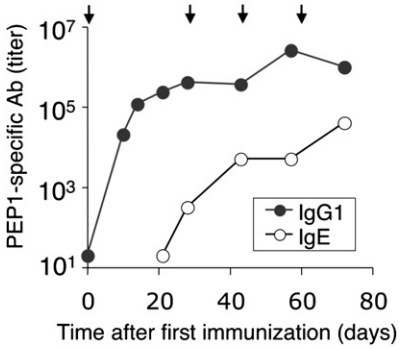

B

		PEP1		HA	
Ig Isotype	Aminoacid	2nd Imm	4th Imm	2nd Imm	4th Imm
IgG1	R^{97}	73	9	94	95
	$R^{97}T$	19	92	0	4
IgE	R^{97}	87	51	89	93
	$R^{97}T$	9	38	0	4
IgG1	N^{100a}	65	19	97	95
	$N^{100a}S/T$	19	66	0	4
IgE	N^{100a}	91	60	95	95
	$N^{100a}S/T$	9	28	0	4
IgG1	A^{101}	84	59	86	88
	$A^{101}T$	11	36	3	0
IgE	A^{101}	91	71	95	86
	$A^{101}T$	4	17	0	5

C

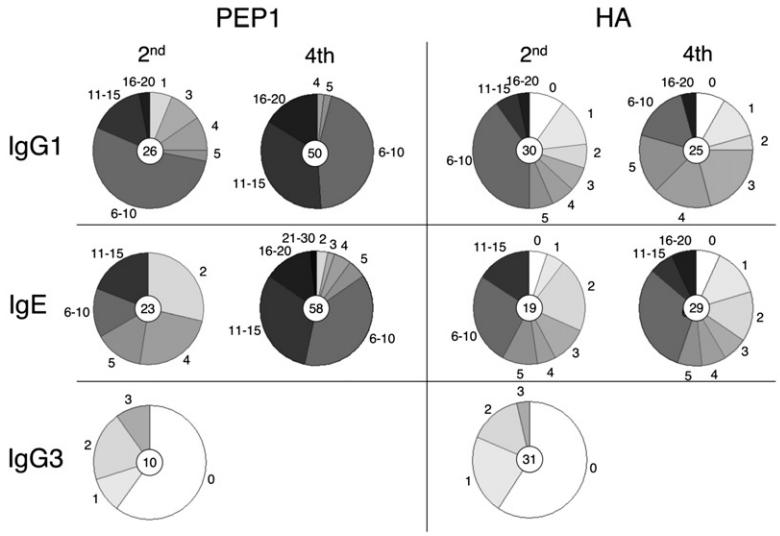

Figure 6. Production of PEP1-Specific IgG1 and IgE Antibodies after Repeated Immunization with OVA-PEP1

(A) T/B monoclonal mice were repeatedly immunized with OVA-PEP1 in alum. Immunization days are indicated by vertical arrows. The serum amounts of PEP1-specific IgG1 and IgE antibodies at the indicated time points were determined by ELISA. n = 5–6 mice per group.

(B) Selection of CDR3 mutations in IgG1 and IgE antibodies of PEP1-immunized mice. Total RNA was extracted from spleen cells of T/B monoclonal mice 10 days after second or fourth immunization with OVA-PEP1 (middle two columns) or OVA-HA (two rightmost columns). IgG1 and IgE VDJ sequences from cDNA were amplified, cloned, and sequenced. The numbers in the boxes represent the percentage of sequences coding for the indicated amino acid residue. The top residue in each box (i.e., R97, N100a, A101) is always the germline residue (Kabat numbering).

(C) Analysis of nucleotide mutations in mice repeatedly immunized with OVA-PEP1 or OVA-HA. The figure shows the proportion of sequences of IgG1, IgE, and IgG3 antibodies carrying the indicated numbers of nucleotide mutations per sequence (shown outside the pies). For each pie, the number of sequences analyzed is written in the center. At least three mice per group and per time point were analyzed. The translated sequences were utilized for the analysis of amino acid mutations shown in (B).

IgG1 molecules, consistent with the results described in Figure 6B. We conclude that memory $IgG1^+$ B cells are able to generate a high-affinity IgE response.

Interleukin-21 Inhibits the Sequential Switching of $IgG1^+$ Cells to IgE

The results shown thus far support a GC origin of mutated IgE antibodies, likely from $IgG1^+$ cells that underwent somatic hypermutation and affinity maturation. However, IgE^+ cells themselves were not found in the GC environment. Some of the factors that can negatively regulate class switching to IgE in the GC are cytokines. Although IL-4 promotes switching to IgE, IL-21, a cytokine produced by follicular T helper cells, inhibits it (Ozaki et al., 2002; Suto et al., 2002; Vinuesa et al., 2005). To assess the effect of IL-21 on sequential switching of $IgG1^+$ cells to IgE, we used an in vitro system. $IgG1^+$ cells and IgD^+ cells were purified from T/B monoclonal mice 10 days after immunization with OVA-HA. Most $IgG1^+$ at day 10 are $GL7^+Fas^+B220^+$ GC cells. The cells were stimulated in vitro with CD40 antibodies, IL-4, and IL-21. The IL-4 concentration used (100 U/ml) is suboptimal to induce

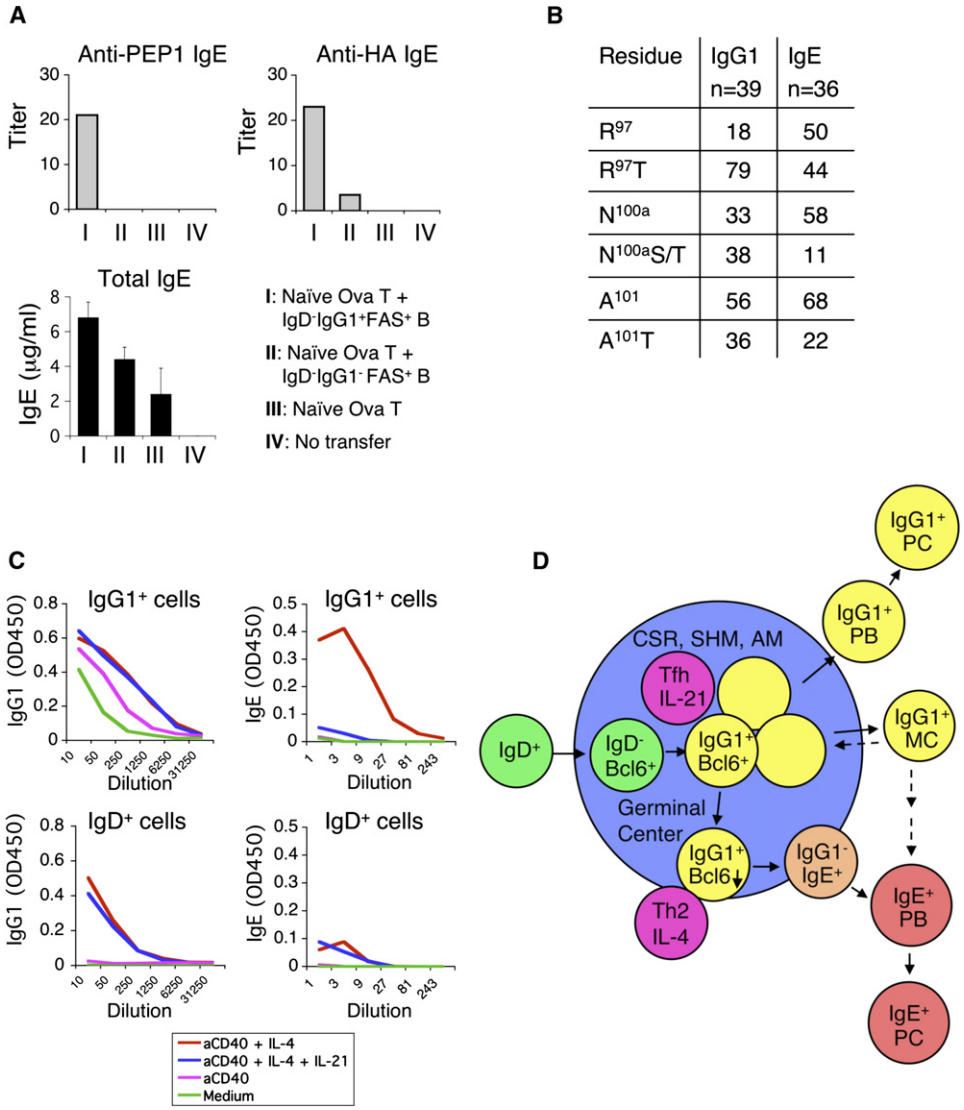

Figure 7. Purified IgG1$^+$ Cells Can Generate High-Affinity IgE Antibodies upon Adoptive Transfer

(A) B220$^+$ IgD$^-$ IgG1$^+$ Fas$^+$ and B220$^+$ IgD$^-$ IgG1$^-$ Fas$^+$ cells were isolated from spleen and lymph nodes of T/B monoclonal mice 20 days after immunization with OVA-PEP1. The purified cells were transferred to TCR$\alpha\beta$-deficient mice together with naive OVA-specific T cells (IgG1$^+$ cells, 8 × 10^5 cells/mouse; IgG1$^-$ cells, 6 × 10^5 cells/mouse; OVA-specific T cells, 5 × 10^5 cells/mouse). The recipient mice, as well as a control groups receiving only T cells or no cells, were immunized with OVA-PEP1 1 day after the transfer. Serum amounts of PEP1-specific, HA-specific, and total IgE were performed on day 13 after immunization. Individual mice were assayed for total IgE (shown average ± SD). HA and PEP1-specific IgE were assayed in IgG-depleted pooled samples. Representative of 3 experiments with n = 3 mice/group.

(B) IgE antibodies derived from sequential switching show hypermutation and selection. B220$^+$IgG1$^+$ cells isolated from mice immunized twice with OVA-PEP1 were transferred together with naive OVA-specific T cells into TCR$\alpha\beta$-deficient recipients. The recipient mice were immunized twice with OVA-PEP1, and the sequences of IgG1 and IgE derived from the transferred B cells were analyzed. VDJ genes derived from donor cells were identified by the knockin VDJ junctional sequence and J_H3 usage. The numbers indicate the percentage of IgG1 or IgE sequences that carry the corresponding mutations.

(C) IL-21 inhibits sequential switching to IgE. IgG1$^+$ cells and IgD$^+$ cells were purified from spleen and LN of T/B monoclonal mice 10 days after i.p. immunization with OVA-HA. Cells were stimulated in vitro with CD40 antibodies (aCD40), IL-4, and IL-21. The figure shows IgE and IgG1 antibody amounts in culture supernatants (day 5). Purified IgD$^+$ cells from nonimmunized mice responded similarly to IgD$^+$ cells from immunized mice. Proliferation was similar in IgD$^+$ and IgG1$^+$ cultures (data not shown). The data shown are representative of three experiments.

(D) A model of the differentiation of IgE$^+$ cells. B lymphocytes in the GC upregulate Bcl6, switch to IgG1, and undergo SHM and affinity maturation. Follicular helper T cells (Tfh) provide an IL-21-rich environment in the GC. Bcl6 expression and signalling through the IL-21R inhibit class switching to IgE in most GC cells. Class switching to IgE can occur in GC cells that downregulate Bcl6 function and interact with Th cells in a high IL-4 and low IL-21 microenvironment. Switching to IgE is linked to a pathway of exit from the GC and differentiation to plasma cell. CSR, class switch recombination; SHM, somatic hypermutation; AM, affinity maturation; PB, plasmablast; PC, plasma cell; MC, memory cell.

CSR to IgE by naive cells but was effective on IgG1$^+$ cells (see below).

IgG1$^+$ cell cultures spontaneously secreted IgG1 antibodies but not IgE antibodies (Figure 7C). Production of IgE in cultures of IgG1$^+$ cells was dependent upon stimulation with CD40 antibodies and IL-4, as indicated by the fact that little or no IgE was produced in nonstimulated cultures or cultures stimulated with CD40 antibodies and no cytokines. IgG1$^+$ cells stimulated with CD40 antibodies plus IL-4 were able to produce much more IgE in these short-term cultures than purified IgD$^+$ cells from naive (not shown) or immunized mice. Switching of IgG1$^+$ cells to IgE was profoundly suppressed by IL-21, whereas IgG1 production was not affected (Figure 7C). These results are consistent with the "de novo" production of IgE by sequential switching of IgG1$^+$ GC cells to IgE in the in vitro cultures. These results are the first demonstration that IL-21 can inhibit the sequential switching of IgG1$^+$ B lymphocytes to IgE.

DISCUSSION

We showed here that IgE$^+$ cells are generated through a unique differentiation pathway of B lymphocytes that differs from the extrafollicular and the follicular GC pathways. Class switching to IgE occurs during the GC phase of a T cell-dependent response, but IgE$^+$ cells are not found in GC and do not express genes typical of the GC stage. Rather, most IgE$^+$ cells express, from early on, a plasma cell program. In spite of their exclusion from GC, IgE$^+$ cells show signs of hypermutation and affinity maturation. We propose a model whereby the high-affinity IgE response is generated by sequential switching of IgG1$^+$ cells, after the latter cells have undergone hypermutation and selection in GC. We provide support for this model by demonstrating that purified IgG1$^+$ cells give rise to IgE antibodies in vivo and in vitro, in a process that is dependent on IL-4 and inhibited by IL-21.

Our data also support the notion that sequential switching from μ to γ1 and from γ1 to ε in vivo does not have to be a temporally continuous event; instead, the two individual recombination steps can be separated by a cellular IgG1$^+$ stage in which cell division, hypermutation, and selection take place in the GC.

It has been demonstrated that in the MRL/lpr background (but not normal background), self-reactive B cells (but not non-self-reactive B cells) undergo somatic hypermutation outside GC (William et al., 2002). It has been also shown that a population of IgM$^+$ human memory B cells carrying mutated receptors can be found in CD40L-deficient patients, who do not harbor normal GC (Weller et al., 2001). Studies in very young children have led to the proposal that receptor diversification in these cells precedes encounter with antigen (Weller et al., 2004). Thus, in these IgM$^+$ B cells, somatic hypermutation appears to occur outside GC and is independent of CD40-CD40L interactions. In contrast, in the case of IgE$^+$ antibodies, all the data shown in this manuscript indicate that the process of somatic hypermutation and affinity maturation takes place in GC, although it appears to occur mostly at the IgG1$^+$ stage. Furthermore, it is known that IgE responses are completely dependent on CD40-CD40L interactions.

CD40-CD40L signaling and the transcription factor Bcl6 are essential for the development of GC, SHM, affinity maturation, and B cell memory (Dent et al., 1997; Foy et al., 1994; Ye et al., 1997). Bcl6 expression has been shown to inhibit transcription through the Iε promoter (Harris et al., 1999). Bcl6 also represses the transcription of Blimp1, a gene whose expression is crucial for plasma cell differentiation (reviewed by Shapiro-Shelef and Calame, 2005). Thus, Bcl6 activity would need to be downregulated in GC cells before the cells could switch to IgE. Our finding that IgE$^+$ cells do not express Bcl6 but express Blimp1 supports the contention that switching to IgE is linked the downregulation of Bcl6, upregulation of Blimp1, and differentiation to plasma cells.

Class switching to IgE depends on IL-4 and is inhibited by IL-21. In GC, IL-21 is produced by follicular Th cells (Tfh). Although the relationship between Th2 cells and Tfh cells is not yet completely understood, it has been reported that, in contrast to Th2 cells, Tfh cells produce little IL-4 (Vinuesa et al., 2005). Our data predicts that CSR to IgE occurs in a GC microenvironment with high IL-4 and low IL-21, perhaps in IgG1$^+$ cells that are exiting GC. The model in Figure 7D summarizes our current view on the generation of high-affinity IgE antibodies through sequential switching of GC IgG1$^+$ cells. Although we found that the majority of IgE$^+$ cells have a PC phenotype, there is a low proportion of IgE$^+$ cells that are B220$^+$ and Syndecan$^-$. IgE$^+$B220$^+$Syn$^-$ cells are observed in both experimental systems that we studied, *Nippostrongylus*-infected mice (15.6% ± 5.0% of IgE$^+$ cells) and OVA-immunized T/B monoclonal mice (8.7% ± 3.3%). Gene-expression studies on the IgE$^+$B220$^+$Syn$^-$ cells showed a GC pattern in both systems. We thus believe that these IgE$^+$B220$^+$Syn$^-$ cells are recently switched cells along the pathway described in this manuscript, although we cannot exclude that they are representative of the conventional GC pathway.

Sequential switching from μ to γ1 to ε in the mouse was discovered when γ1 remnants were found in μ-ε switch regions (Yoshida et al., 1990), a report that has since been confirmed by numerous studies in both human and mouse IgE$^+$ cells. By using a mouse strain unable to produce IgG1 antibodies because of a deletion in the Sγ1 region, Jung et al. showed that sequential switching was not essential for the production of IgE antibodies (Jung et al., 1994). However, the affinity maturation of the IgE reponse in these mice, which cannot generate IgE antibodies through sequential switching, was not determined. Our experiments shed new light on to the process of sequential switching and its biological importance. First, we showed that sequential switching entails two recombination processes that can be separated in time, having an intermediate IgG1$^+$ cellular phase. Second, we showed that sequential switching to IgE in vivo is linked to plasma cell differentiation. Third, we showed that sequential switching of GC and memory IgG1$^+$ cells allowed the production of

high-affinity IgE antibodies without the need for an extended IgE^+ GC phase.

We showed that $IgG1^+IgE^+$ dual-expressing cells have a plasma cell phenotype, despite their coexpression of IgG1. This result excludes the possibility that the paucity of IgE^+ cells in GC is the result of unfavorable competition with $IgG1^+$ cells. It has been shown that the unique cytoplasmic domains of the different immunoglobulins are critical for signaling (Achatz et al., 1997; Kaisho et al., 1997; Manser, 2002; Martin and Goodnow, 2002). It was thus possible that cells switching to IgE within GC would not be able to compete with $IgG1^+$ cells because of a less effective signaling or interiorization capacity of IgE cytoplasmic domains. In contrast, the results with the dual-expressing cells further strengthen the programmatic link between switching to IgE and plasma cell differentiation.

During primary T cell-dependent responses, two main phases of B cell activation have been described (MacLennan et al., 1997). Early activation and CSR occur often in extrafollicular foci, producing short-lived plasma cells that secrete low-affinity antibodies and generate no memory. A second phase occurs in GCs, where CSR, SHM, and affinity maturation take place. GC reactions generate long-lived plasma cells and memory B cells with high-affinity mutated BCR. Memory B cells differentiate into plasma cells upon new antigenic encounter, producing high-affinity antibodies. IgE^+ cells do not conform to either the pre-GC (primary foci) or the GC maturation pattern. IgE class switching coincides temporarily with GC and appears to take place in the GC, but IgE^+ cells are found outside GC. The short or inexistent IgE^+ GC phase, together with lack of expression of GC genes such as AID by IgE^+ cells, appear incompatible with SHM and selection. However, high-affinity IgE antibodies are produced, and here we provide evidence that they can be derived from sequential switching of high-affinity $IgG1^+$ cells. This model thus predicts that high-affinity IgE antibodies are generated mainly through sequential switching whereas direct switching from IgM to IgE generates low-affinity IgE. The importance of the sequential switching pathway in the generation of the high-affinity IgE response is strengthened by the paucity of cells with a bona fide memory phenotype among IgE^+ cells.

EXPERIMENTAL PROCEDURES

Mice, Immunization, and Infection

T/B monoclonal mice were obtained by crossing the 17/9 immunoglobulin knockin mice with DO11.10 TCR transgenic mice and with *RAG1*$^{-/-}$ mice (Curotto de Lafaille et al., 2001) and were backcrossed to the BALB/c genetic background. Heterozygous heavy and light chain knockin mice were used in all experiments, except in the experiments described in Figure 4, in which homozygous knockin mice were used. T/B monoclonal mice were immunized by intraperitoneal injection of 100 μg of OVA-HA (chicken ovalbumin crosslinked to the HA peptide YPYDVPDYASLRS) or with 100 μg OVA-PEP1 (chicken ovalbumin crosslinked to the PEP1 peptide YPYDVPDFASLRS) in alum. BALB/c mice were infected with 200 L3 larvae of *Nippostrongylus brasiliensis* via subcutaneous route (Katona et al., 1988).

All procedures involving mice were approved by New York University's Institutional and Animal Care Use Committee (IACUC).

Immunohistology

Spleen and LN were frozen in Oct compound (Tissue-Tek) and sectioned with a MICROM Vacutom (8–10 μm sections). The sections were treated for 1 min with acid buffer (0.085 M NaCl, 0.005 M KCl, 0.01 M EDTA, and 0.05 M NaAcetate [pH 4]) to remove cytophilic (extrinsic, CD23-bound) antibodies (Katona et al., 1983, 1985), then neutralized with PBS, fixed in acetone, and incubated 1 hr in blocking buffer (PBS with 2% BSA and 20 μg/ml of CD16/32 antibodies). The sections were incubated overnight at 4°C for primary staining and 1 hr at 4°C for secondary staining. Images were acquired with an Axioplan 2 fluorescent Microscope (Zeiss). Reagents: biotin- and FITC-IgE (R35-72), biotin-anti-IgG1 (A85-1), FITC-anti-IgD (11-26c 2a), APC-anti-TCRβ (H57-597), and FITC-GL7 were purchased from BD Pharmingen. APC-anti-B220 (RA3-6B2), PE-KJ1-26, Cy3-Streptavidin, and Cy-5-Streptavidin were purchased from Caltag.

Flow Cytometry

Before staining for FACS analysis, single-cell suspensions from spleen and mesenteric LN were treated for 1 min with ice-cold acid buffer (paragraph above) to remove extrinsic IgE antibodies noncovalently bound to CD23. The samples were then neutralized with a large volume of cell-culture medium and washed twice before staining. The following reagents were used: FITC-anti-IgG1 (A85-1), biotin-anti-IgE (R35-72), PerCP-anti-B220 (RA3-6B2), PE-anti Fas (jo2), PE-anti-Syndecan-1 (281-2), and APC-Streptavidin (BD Pharmingen).

Real-Time PCR

For cytometer sorting (MoFlo, Cytomation, CO) of GC and non-GC populations (Figure 3), spleen cells were stained with APC-anti-B220 (Caltag), FITC-PNA (Vector), biotin-anti-IgG1, PE-anti-Syndecan-1, and PE-Cy7-Streptavidin (BD Pharmingen). Total RNA extraction and cDNA synthesis was performed by standard procedures. Real-time PCR on cDNA samples was performed with the following primers: ε sterile transcript: CACAGGGGGCAGAAGATG and AGGGGTAGAG CTGAGGGTTC; ε switched transcript: CTCTGGCCCTGCTTATTGTTG (Muramatsu et al., 2000) and AGTTCACAGTGCTCATGTTCAG (IgE2); ε mature transcript: TACGACGAGAACGGGTTTGCTTAC and IgE2. β-actin amplification was used for normalization in all real-time PCR analysis (Curotto de Lafaille et al., 2004).

For the real-time PCR analysis shown in Figures 4 and 5, acid-treated spleen and LN cells were stained with APC-anti-B220, biotin-anti-IgG1, PE-anti-Fas, FITC-anti-IgE, and PE-Cy7-Streptavidin and sorted in a MoFlo cytometer. Naive $B220^+$ cells were isolated from untreated T/B monoclonal mice by magnetic sorting with Miltenyi reagents. The following primers were used for real-time PCR on cDNA samples: Pax5, AACCCATCAAGCCAGAACAG and GGCCTCC AGCCAGTGAAG; Bcl6, CTTCCGCTACAAGGGCAAC and TCGAGTG TGGGTCTTCAGG; AID, GACGGCATGAGACCTACCTC and GTGGCA GCCAGACTTGTTG; Blimp1, TGGTATTGTCGGGACTTTGC and TGG GGACACTCTTTGGGTAG; Xbp1, GGAGTGGAGTAAGGCTGGTG and ATGTTCTGGGGAGGTGACAA; CXCR5, ATGCTACTTCCCTCACCACC and TCCTCCCAAGGAAAACAGAA.

VDJ Sequence Analysis

Total RNA extraction and cDNA synthesis were performed by standard procedures. PCR reactions were performed with ExTaq Polymerase (TaKaRa) and the primer 5′UTR (CAGTCAGCACTGAACACGGACC) in combination with primers specific for IgE (GCCTTTACAGGGCTTT AAG), IgG1 (GGATCCAGAGTTCCAGGTCACT), or IgG3 (CATAGTTC CATTTTACAGTTACC) constant regions. The PCR products were cloned (TA cloning kit; Invitrogen) and sequenced.

ELISA

Total and antigen-specific IgE and IgG1 antibodies were quantified by ELISA as described (Curotto de Lafaille et al., 2001). To measure antigen-specific IgE, pooled serum samples from each group were first depleted of IgG antibodies by incubation with GammaBind Plus Sepharose (Amersham Biosciences).

Adoptive Transfer of IgG1$^+$ Cells

B220$^+$IgD$^-$IgG1$^+$Fas$^+$ and B220$^+$IgD$^-$IgG1$^-$Fas$^+$ cells were purified by cytometer sorting (MoFlo) from pooled spleen and mesenteric lymph nodes of T/B monoclonal mice immunized with OVA-PEP1. The purified cells were transferred to *TCR*$\alpha\beta^{-/-}$ mice together with naive OVA-specific T cells, or to DO11.10 TCR transgenic *RAG1*$^{-/-}$ mice. The recipient mice, as well as control mice, were immunized with 100 μg OVA-PEP1 in alum 1 day after the transfer. IgE and IgG1 antibody levels in serum were determined by ELISA. Sequence analysis of IgG1 and IgE antibodies was performed as described above.

Sequential Switching In Vitro

B220$^+$IgG1$^+$ cells and B220$^+$IgD$^+$ cells were purified by flow cytometry sorting (MoFlo) from spleen and LN of OVA-HA-immunized T/B monoclonal mice. Cells were stimulated in vitro with CD40 antibodies (3 μg/ml; clone HM40-3, BD Pharmingen), IL-4 (100 U/ml; BD Pharmingen), and IL-21 (30 ng/ml; R&D). The IL-4 concentration was purposely used at suboptimal level for IgE production by naive cells. In our hands, optimal stimulation for IgE production requires 500 U/ml of IL-4. 48 hr and 5 days after B cell stimulation, the supernatants were collected and IgE and IgG1 antibody levels were determined by ELISA. High IgE production was detected at 48 hr only in cultures of IgG1$^+$ cells stimulated with CD40 antibodies and IL-4.

Supplemental Data

Ten Supplemental Figures can be found with this article online at http://www.immunity.com/cgi/content/full/26/2/191/DC1/.

ACKNOWLEDGMENTS

We thank D. Littman, D. Roth, J. Cyster, S. Shen, and V. Brandt for critically reading the manuscript. Work in J.J.L. laboratory is supported by the NIH/NAIAD, the National Multiple Sclerosis Society, and the Dana-Goldsmith Foundation.

Received: May 7, 2006
Revised: December 4, 2006
Accepted: December 13, 2006
Published online: February 8, 2007

REFERENCES

Achatz, G., Nitschke, L., and Lamers, M.C. (1997). Effect of transmembrane and cytoplasmic domains of IgE on the IgE response. Science *276*, 409–411.

Allen, C.D., Ansel, K.M., Low, C., Lesley, R., Tamamura, H., Fujii, N., and Cyster, J.G. (2004). Germinal center dark and light zone organization is mediated by CXCR4 and CXCR5. Nat. Immunol. *5*, 943–952.

Coffman, R.L., Lebman, D.A., and Rothman, P. (1993). Mechanism and regulation of immunoglobulin isotype switching. Adv. Immunol. *54*, 229–270.

Curotto de Lafaille, M.A., Muriglan, S., Sunshine, M.J., Lei, Y., Kutchukhidze, N., Furtado, G.C., Wensky, A.K., Olivares-Villagomez, D., and Lafaille, J.J. (2001). Hyper immunoglobulin E response in mice with monoclonal populations of B and T lymphocytes. J. Exp. Med. *194*, 1349–1359.

Curotto de Lafaille, M.A., Lino, A.C., Kutchukhidze, N., and Lafaille, J.J. (2004). CD25- T cells generate CD25+Foxp3+ regulatory T cells by peripheral expansion. J. Immunol. *173*, 7259–7268.

Cyster, J.G. (1999). Chemokines and cell migration in secondary lymphoid organs. Science *286*, 2098–2102.

Dent, A.L., Shaffer, A.L., Yu, X., Allman, D., and Staudt, L.M. (1997). Control of inflammation, cytokine expression, and germinal center formation by BCL-6. Science *276*, 589–592.

Finkelman, F.D., Katona, I.M., Urban, J.F., Jr., Holmes, J., Ohara, J., Tung, A.S., Sample, J.V., and Paul, W.E. (1988). IL-4 is required to generate and sustain in vivo IgE responses. J. Immunol. *141*, 2335–2341.

Finkelman, F.D., Holmes, J., Urban, J.F., Jr., Paul, W.E., and Katona, I.M. (1989). T help requirements for the generation of an in vivo IgE response: a late acting form of T cell help other than IL-4 is required for IgE but not for IgG1 production. J. Immunol. *142*, 403–408.

Finkelman, F.D., Holmes, J., Katona, I.M., Urban, J.F., Jr., Beckmann, M.P., Park, L.S., Schooley, K.A., Coffman, R.L., Mosmann, T.R., and Paul, W.E. (1990). Lymphokine control of in vivo immunoglobulin isotype selection. Annu. Rev. Immunol. *8*, 303–333.

Foy, T.M., Laman, J.D., Ledbetter, J.A., Aruffo, A., Claassen, E., and Noelle, R.J. (1994). gp39-CD40 interactions are essential for germinal center formation and the development of B cell memory. J. Exp. Med. *180*, 157–163.

Gonda, H., Sugai, M., Nambu, Y., Katakai, T., Agata, Y., Mori, K.J., Yokota, Y., and Shimizu, A. (2003). The balance between Pax5 and Id2 activities is the key to AID gene expression. J. Exp. Med. *198*, 1427–1437.

Harris, M.B., Chang, C.C., Berton, M.T., Danial, N.N., Zhang, J., Kuehner, D., Ye, B.H., Kvatyuk, M., Pandolfi, P.P., Cattoretti, G., et al. (1999). Transcriptional repression of Stat6-dependent interleukin-4-induced genes by BCL-6: specific regulation of iepsilon transcription and immunoglobulin E switching. Mol. Cell. Biol. *19*, 7264–7275.

Hoshino, T., Yagita, H., Ortaldo, J.R., Wiltrout, R.H., and Young, H.A. (2000). In vivo administration of IL-18 can induce IgE production through Th2 cytokine induction and up-regulation of CD40 ligand (CD154) expression on CD4+ T cells. Eur. J. Immunol. *30*, 1998–2006.

Johnson, K., and Calame, K. (2003). Transcription factors controlling the beginning and end of B-cell differentiation. Curr. Opin. Genet. Dev. *13*, 522–528.

Jung, S., Siebenkotten, G., and Radbruch, A. (1994). Frequency of immunoglobulin E class switching is autonomously determined and independent of prior switching to other classes. J. Exp. Med. *179*, 2023–2026.

Kaisho, T., Schwenk, F., and Rajewsky, K. (1997). The roles of gamma 1 heavy chain membrane expression and cytoplasmic tail in IgG1 responses. Science *276*, 412–415.

Kaplan, M.H., Schindler, U., Smiley, S.T., and Grusby, M.J. (1996). Stat6 is required for mediating responses to IL-4 and for development of Th2 cells. Immunity *4*, 313–319.

Katona, I.M., Urban, J.F., Jr., Scher, I., Kanellopoulos-Langevin, C., and Finkelman, F.D. (1983). Induction of an IgE response in mice by *Nippostrongylus brasiliensis*: characterization of lymphoid cells with intracytoplasmic or surface IgE. J. Immunol. *130*, 350–356.

Katona, I.M., Urban, J.F., Jr., and Finkelman, F.D. (1985). B cells that simultaneously express surface IgM and IgE in *Nippostrongylus brasiliensis*-infected SJA/9 mice do not provide evidence for isotype switching without gene deletion. Proc. Natl. Acad. Sci. USA *82*, 511–515.

Katona, I.M., Urban, J.F., Jr., and Finkelman, F.D. (1988). The role of L3T4+ and Lyt-2+ T cells in the IgE response and immunity to *Nippostrongylus brasiliensis*. J. Immunol. *140*, 3206–3211.

Kuhn, R., Rajewsky, K., and Muller, W. (1991). Generation and analysis of interleukin-4 deficient mice. Science *254*, 707–710.

Li, S.C., Rothman, P.B., Zhang, J., Chan, C., Hirsh, D., and Alt, F.W. (1994). Expression of I mu-C gamma hybrid germline transcripts subsequent to immunoglobulin heavy chain class switching. Int. Immunol. *6*, 491–497.

MacLennan, I.C., Gulbranson-Judge, A., Toellner, K.M., Casamayor-Palleja, M., Chan, E., Sze, D.M., Luther, S.A., and Orbea, H.A. (1997). The changing preference of T and B cells for partners as T-dependent antibody responses develop. Immunol. Rev. *156*, 53–66.

Manser, T. (2002). Effector BCRs: inside information on IgG. Nat. Immunol. *3*, 114–116.

Martin, S.W., and Goodnow, C.C. (2002). Burst-enhancing role of the IgG membrane tail as a molecular determinant of memory. Nat. Immunol. *3*, 182–188.

Muramatsu, M., Kinoshita, K., Fagarasan, S., Yamada, S., Shinkai, Y., and Honjo, T. (2000). Class switch recombination and hypermutation require activation-induced cytidine deaminase (AID), a potential RNA editing enzyme. Cell *102*, 553–563.

Oettgen, H.C., and Geha, R.S. (2001). IgE regulation and roles in asthma pathogenesis. J. Allergy Clin. Immunol. *107*, 429–440.

Ozaki, K., Spolski, R., Feng, C.G., Qi, C.F., Cheng, J., Sher, A., Morse, H.C., 3rd, Liu, C., Schwartzberg, P.L., and Leonard, W.J. (2002). A critical role for IL-21 in regulating immunoglobulin production. Science *298*, 1630–1634.

Pinilla, C., Appel, J.R., and Houghten, R.A. (1993). Functional importance of amino acid residues making up peptide antigenic determinants. Mol. Immunol. *30*, 577–585.

Przylepa, J., Himes, C., and Kelsoe, G. (1998). Lymphocyte development and selection in germinal centers. Curr. Top. Microbiol. Immunol. *229*, 85–104.

Rabbitts, T.H., Forster, A., Dunnick, W., and Bentley, D.L. (1980). The role of gene deletion in the immunoglobulin heavy chain switch. Nature *283*, 351–356.

Reimold, A.M., Iwakoshi, N.N., Manis, J., Vallabhajosyula, P., Szomolanyi-Tsuda, E., Gravallese, E.M., Friend, D., Grusby, M.J., Alt, F., and Glimcher, L.H. (2001). Plasma cell differentiation requires the transcription factor XBP-1. Nature *412*, 300–307.

Rothman, P., Lutzker, S., Cook, W., Coffman, R., and Alt, F.W. (1988). Mitogen plus interleukin 4 induction of C epsilon transcripts in B lymphoid cells. J. Exp. Med. *168*, 2385–2389.

Schulze-Gahmen, U., Rini, J.M., and Wilson, I.A. (1993). Detailed analysis of the free and bound conformations of an antibody. X-ray structures of Fab 17/9 and three different Fab-peptide complexes. J. Mol. Biol. *234*, 1098–1118.

Shapiro-Shelef, M., and Calame, K. (2005). Regulation of plasma-cell development. Nat. Rev. Immunol. *5*, 230–242.

Shih, T.A., Meffre, E., Roederer, M., and Nussenzweig, M.C. (2002). Role of BCR affinity in T cell dependent antibody responses in vivo. Nat. Immunol. *3*, 570–575.

Shimoda, K., van Deursen, J., Sangster, M.Y., Sarawar, S.R., Carson, R.T., Tripp, R.A., Chu, C., Quelle, F.W., Nosaka, T., Vignali, D.A., et al. (1996). Lack of IL-4-induced Th2 response and IgE class switching in mice with disrupted Stat6 gene. Nature *380*, 630–633.

Stavnezer, J., Radcliffe, G., Lin, Y.C., Nietupski, J., Berggren, L., Sitia, R., and Severinson, E. (1988). Immunoglobulin heavy-chain switching may be directed by prior induction of transcripts from constant-region genes. Proc. Natl. Acad. Sci. USA *85*, 7704–7708.

Suto, A., Nakajima, H., Hirose, K., Suzuki, K., Kagami, S., Seto, Y., Hoshimoto, A., Saito, Y., Foster, D.C., and Iwamoto, I. (2002). Interleukin 21 prevents antigen-induced IgE production by inhibiting germ line C(epsilon) transcription of IL-4-stimulated B cells. Blood *100*, 4565–4573.

Vinuesa, C.G., Tangye, S.G., Moser, B., and Mackay, C.R. (2005). Follicular B helper T cells in antibody responses and autoimmunity. Nat. Rev. Immunol. *5*, 853–865.

Weller, S., Faili, A., Garcia, C., Braun, M.C., Le Deist, F.F., de Saint Basile, G.G., Hermine, O., Fischer, A., Reynaud, C.A., and Weill, J.C. (2001). CD40-CD40L independent Ig gene hypermutation suggests a second B cell diversification pathway in humans. Proc. Natl. Acad. Sci. USA *98*, 1166–1170.

Weller, S., Braun, M.C., Tan, B.K., Rosenwald, A., Cordier, C., Conley, M.E., Plebani, A., Kumararatne, D.S., Bonnet, D., Tournilhac, O., et al. (2004). Human blood IgM "memory" B cells are circulating splenic marginal zone B cells harboring a prediversified immunoglobulin repertoire. Blood *104*, 3647–3654.

William, J., Euler, C., Christensen, S., and Shlomchik, M.J. (2002). Evolution of autoantibody responses via somatic hypermutation outside of germinal centers. Science *297*, 2066–2070.

Ye, B.H., Cattoretti, G., Shen, Q., Zhang, J., Hawe, N., de Waard, R., Leung, C., Nouri-Shirazi, M., Orazi, A., Chaganti, R.S., et al. (1997). The BCL-6 proto-oncogene controls germinal-centre formation and Th2-type inflammation. Nat. Genet. *16*, 161–170.

Yoshida, K., Matsuoka, M., Usuda, S., Mori, A., Ishizaka, K., and Sakano, H. (1990). Immunoglobulin switch circular DNA in the mouse infected with *Nippostrongylus brasiliensis*: evidence for successive class switching from mu to epsilon via gamma 1. Proc. Natl. Acad. Sci. USA *87*, 7829–7833.

Yoshimoto, T., Mizutani, H., Tsutsui, H., Noben-Trauth, N., Yamanaka, K., Tanaka, M., Izumi, S., Okamura, H., Paul, W.E., and Nakanishi, K. (2000). IL-18 induction of IgE: dependence on CD4+ T cells, IL-4 and STAT6. Nat. Immunol. *1*, 132–137.